AN APPLICATION OF FINITE ELEMENT ANALYSIS TO WOOD DRYING

Young Q. Gui

Postdoctoral Assistant
Mississippi Forest Products Lab

E. William Jones

Professor
Department of Mechanical Engineering

Fred W. Taylor

Professor
Mississippi Forest Products Lab

and

Camille A. Issa

Associate Professor
Department of Engineering Mechanics

Mississippi State University
Mississippi State, MS 39762

(Received April 1992)

ABSTRACT

Because of the nonhomogeneous and nonlinear properties of wood, exact solutions for heat and mass transfer are difficult to obtain by current methods of analysis. This work presents a numerical solution for the analysis of drying wood using the finite element method. A nonlinear model was established on a two-dimensional finite element grid structure that considers local density variation. Through the finite element method of analysis of unsteady-state heat and moisture transfer in wood, the dynamic profiles of temperature and moisture content were determined at a series of drying times. The resulting numerical solutions match well with experimental results and with published results. The results will help to extend understanding of wood-water and temperature relations. In future studies, these data can be incorporated into drying stress analysis to analyze checking or warping.

Keywords: Mass transfer, heat transfer, moisture content, temperature, spruce, southern pine, *Pinus* spp., wood drying, numerical analysis, finite element method.

NOMENCLATURE

T = wood temperature, K
T_{air} = temperature of drying air, K
T_0 = initial wood temperature, K
T_s = wood surface temperature, K
M = wood moisture potential, °M
M_{air} = moisture potential of drying air, °M
M_0 = initial wood moisture potential, °M
M_s = wood surface moisture potential, °M
ρ = dry body density, kg/m^3
C_q = heat capacity, J/kg·K
C_m = moisture capacity, kg (moisture)/kg (dry body)·°M
α_q = convective heat transfer coefficient, W/m^2·K
α_m = convective mass transfer coefficient, kg/m^2·sec·°M
K_{qq} = thermal transfer coefficient, W/m·K
K_{mm} = mass transfer coefficient, kg/m·sec·°M
K_{qm} = heat transfer coefficient due to mass gradient, J/m·sec·°M

Wood and Fiber Science, 26(2), 1994, pp. 281–293

K_{mq} = mass transfer coefficient due to temperature gradient, kg/m·sec·K
t = drying time, second
$\nabla^2 = \left(\frac{\partial^2}{\partial x^2} + \frac{\partial^2}{\partial y^2}\right)$, Laplacian operator
$\nabla = \left(\frac{\partial}{\partial x} + \frac{\partial}{\partial y}\right)$, gradient
$\{Q\}$ = heat flow rate vector
$\{H\}$ = mass flow rate vector
$\{T\}$ = temperature vector
$\{\dot{T}\}$ = time derivative of temperature vector
$\{M\}$ = mass vector
$\{\dot{M}\}$ = time derivative of mass vector
$[K]$ = conductivity matrix
$[B]$ = temperature gradient interpolation matrix

INTRODUCTION

In the process of manufacturing lumber, drying is the single most costly step in terms of energy consumption and time. A reduction in drying time or an increase in the quality of the dried lumber offers potential economic benefit. Improvements in the wood drying process will be facilitated by a greater understanding of the drying process and by development of a quantitative method to determine the relationships of factors involved in drying rate.

Using mathematical models to simulate wood drying is a recognized means for improving kiln schedules (Ashworth 1979; Hart 1981; Lessard 1982a, b; Spolek and Plumb 1980). Three major advantages of using predictive mathematical models are: the sensitivity of the model's response to changes in drying parameters can be easily evaluated; the solution can be generalized among different wood species; and the relationships between wood, water, and temperature can be analyzed. Changes in temperature and moisture gradients during drying have been incorporated into mechanical models to analyze drying-induced stresses and defects (Ashworth 1979; Kawai et al. 1979; Lessard 1982b; Lewis et al. 1979; Moren 1989; Morgan et al. 1982). Because of the complexity of mathematical transport models, analytical solutions exist for only extremely simple problems, and numerical solutions are difficult to obtain if simplifying assumptions are not made. Moreover, variation in wood density could affect moisture transfer and distribution. Above the fiber saturation point, peaks in moisture content can coincide with valleys in density and vice versa. This density influence on mass transfer has been found and reported (Plumb et al. 1984; Northway 1989).

The finite element method (FEM) is a numerical technique for solving partial differential equations applying to many physical phenomena. This method was developed for mechanical structural analysis but has been adopted to solve other continuum problems. The FEM analysis of continua lends itself to the study of wood since the whole material may be divided into small elements of material with each element having different values of density, thermal conductivity, moisture conductivity, etc. A finite element mesh that includes gradients or property differences should yield a reasonably accurate solution, especially for woods, such as pine, with abrupt property differences between earlywood and latewood.

This study uses the finite element method of analysis to examine the dynamic changes of heat and mass transfer in wood drying. Historically, mathematical models have ignored variations in wood density and other physical properties that affect moisture movement. This study attempts to simplify published numerical models and to improve the accuracy of numerical prediction by considering density variation along the growth rings. The numerical solutions of a mathematical model are compared with experimental data and previously published results. Two species, spruce and southern pine (*Pinus* spp.), were analyzed to test the reliability of the simplified mathematical model and the adaptability of the FEM. The influence of the pattern of earlywood and latewood on moisture content and temperature distribution was investigated.

HEAT AND MOISTURE TRANSFER THROUGH WOOD

Governing equations

A number of mathematical models have been developed to describe the characteristics of wood drying. Most models involve second-order spatial derivatives and first-order time derivatives. "Advances in Drying" (edited by Mujumdar, 1980–1987) provides a good review of mathematical models for heat and mass transfer.

In this study, the physical dimensions of the wood samples had a length to width ratio of 20:1; hence the longitudinal flows of heat and moisture are negligible relative to the transverse flow rates (Siau 1984). On the basis of the thermodynamics of irreversible processes, Luikov (1964, 1966, 1975) and Lukov and Mikhailov (1965) developed a coupled system of partial differential governing equations for heat and mass transfer in porous bodies:

$$\rho C_q \frac{\partial T}{\partial t} = K_{qq}\nabla^2 T + K_{qm}\nabla^2 M, \qquad (1)$$

and

$$\rho C_m \frac{\partial M}{\partial t} = K_{mq}\nabla^2 T + K_{mm}\nabla^2 M. \qquad (2)$$

The two-dimensional Luikov equations have been solved using the FE method to predict the temperature and moisture distributions in lumber during drying (Lewis et al. 1979; Morgan et al. 1982; Thomas et al. 1980). The results of this study will be compared to those investigations.

The governing equations include the Dufour effect ($K_{qm}\nabla^2 M$) and the Soret effect ($K_{mq}\nabla^2 T$). The analytical solution of these equations presents great mathematical difficulties, and few solutions have been obtained for simple geometrical and boundary conditions (Luikov and Mikhailov 1965; Liu and Cheng 1989). These difficulties hinder the utilization of the mathematical models. Usually, the Dufour effect and the Soret effect have small influences on the overall transport of heat and mass. A simplification was achieved by merging the coupling coefficients K'_{qq} and K'_{mm} into the main transport terms through Egner's method (1934). With this procedure, the mass and heat transfer processes can be analyzed separately. When these combined coupling coefficients are applied to Eqs. (1) and (2), the resulting equations are:

$$\rho C_q \frac{\partial T}{\partial t} = \nabla(K'_{qq}\nabla T), \qquad (3)$$

and

$$\rho C_m \frac{\partial M}{\partial t} = \nabla(K'_{mm}\nabla M). \qquad (4)$$

In the governing equation for mass transfer, moisture potential is the driving force and is analogous to heat potential (temperature). Also, moisture capacity is analogous to heat capacity, as detailed in Luikov's book (1966). Both potentials are termed the thermodynamic potentials or affinities. The moisture potential M is related to moisture content, m, by

$$m = C_m M. \qquad (5)$$

At the wood surface, the boundary conditions are

$$K'_{qq}\nabla T + \alpha_q(T_s - T_{air}) = 0, \qquad (6)$$

and

$$K'_{mm}\nabla M + \alpha_m(M_s - M_{air}) = 0. \qquad (7)$$

Because of symmetry, conditions at the wood's center are

$$\frac{\partial T}{\partial x} = 0, \qquad \frac{\partial T}{\partial y} = 0 \qquad (8)$$

and

$$\frac{\partial M}{\partial x} = 0, \qquad \frac{\partial M}{\partial y} = 0. \qquad (9)$$

The initial conditions throughout the board are assumed to be constant:

$$T(X, Y, t) = T(X, Y, 0) = T_0, \qquad (10)$$

and

$$M(X, Y, t) = M(X, Y, 0) = M_0. \qquad (11)$$

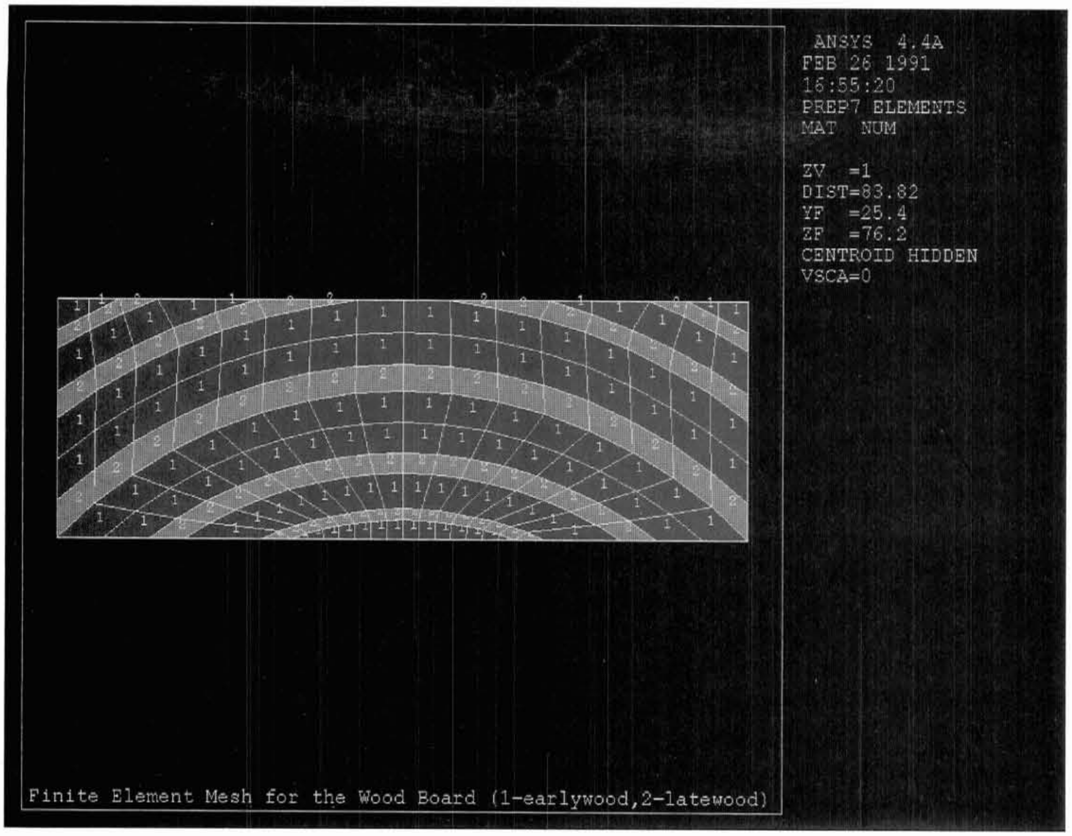

FIG. 1. FEM mesh for heat and mass transfer in wood.

Transport coefficient data

The FEM has been used with some success to analyze heat and mass transfer in wood drying (Felixx et al. 1989; Moren 1989; Morgan et al. 1982; Thomas et al. 1980). However, the thermophysical parameters should be variables in unsteady-state transport, especially when moisture content varies above and below the fiber saturation point (Siau 1984; Skaar 1954, 1988). Therefore, consideration was given to transport coefficient changes over the whole range of the drying and also to wood density variations in Eqs. (3) and (4) for the unsteady-state transport.

Egner's method (1934) used a form of Fick's law to determine the variable transport coefficients and does not require special limitations or assumptions. This is an advantage over other methods for obtaining the real dynamic transport coefficient over the whole range of drying. This method has been successfully used by researchers in the previous finite difference method of analysis (Kawai et al. 1979; Rice 1988). In Egner's method, the cumulative flux is represented by the difference in areas under the moisture distribution curves. The changes in the areas reflect all possible variables that are related to heat and mass transfer in wood. The transport coefficients, K'_{mm} and K'_{qq}, will be determined from experimental data by using Egner's method.

NUMERICAL ANALYSIS

In this study, a finite element mesh was developed that models the growth ring curvature with the difference in earlywood and latewood properties (Fig. 1). A finite element software, ANSYS[1], was used to carry out the numerical calculations of the transfer governing equations.

The FEM of analysis breaks the solution domain into small, discrete regions called elements, which have nodal points or nodes that lie along the boundary to represent the original continuous system. Values of temperature and moisture content at each node are designated as $\{T_e\}$ and $\{M_e\}$. Values of temperature or moisture content between nodes are evaluated by shape functions $\{N\}$. The shape functions are polynomial expressions of temperature or moisture content that express $\{T\}$ and $\{M\}$ as functions of position between the nodes and the nodal values of $\{T_e\}$ and $\{M_e\}$. Since mass transfer is analogous to heat transfer, the following formulations are given for heat transfer.

The shape function for the two-dimensional isoparametric solid element (Kohnke 1989) with four nodes and local coordinates s and t is:

$$\{N\} = 1/4[(1 - s)(1 - t)\ (1 + s)(1 - t)\cdot \cdot(1 + s)(1 + t)\ (1 - s)(1 + t)]. \tag{12}$$

The values for temperature at the I_{th}, J_{th}, K_{th} and L_{th} nodes of the element are:

$$\{T_e\} = \{T_I T_J T_K T_L\}^T. \tag{13}$$

The values for the temperature field between the nodes are defined by those values at the nodes and the shape function.

The temperature at any location x, y within this element is:

$$T(x, y) = \{N\}\{T_e\}. \tag{14}$$

Temperature gradients are:

$$\left\{\begin{matrix} \dfrac{\partial T(x, y)}{\partial x} \\ \dfrac{\partial T(x, y)}{\partial y} \end{matrix}\right\} = [B]\{T_e\}, \tag{15}$$

[1] ANSYS is a registered trademark of Swanson Analysis Systems, Inc.

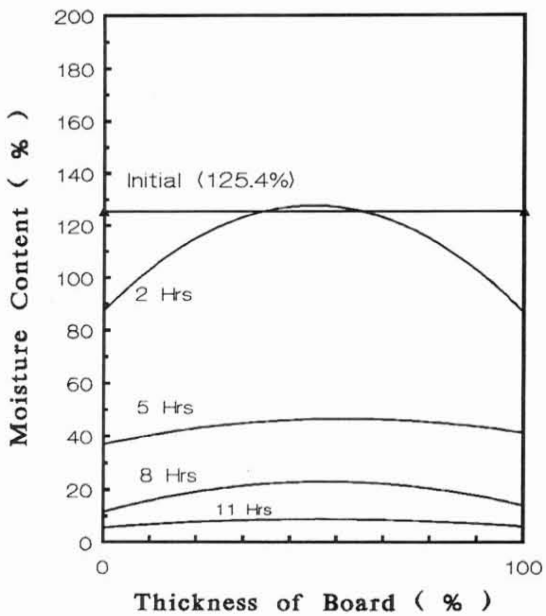

FIG. 2. Moisture gradients (radial direction) measured during drying of southern pine.

where the temperature gradient interpolation matrix [B] is:

$$[B] = \begin{bmatrix} \left\{\dfrac{\partial N}{\partial x}\right\}^T \\ \left\{\dfrac{\partial N}{\partial y}\right\}^T \end{bmatrix}. \tag{16}$$

The temperature conductivity matrix relates nodal values of $\{T_e\}$ for the interior of the element as follows:

$$[K_e^B] = \int_{vol} [B]^T[K][B]\, d(vol). \tag{17}$$

For conductivity at the convection surface:

$$[K_e^S] = \alpha \int_{area} \{N|_s\}\{N|_s\}^T\, d(area). \tag{18}$$

For the specific heat or moisture matrix:

$$[C_e] = \rho C \int_{vol} \{N\}\{N\}^T\, d(vol). \tag{19}$$

For the total element heat flow vector:

$$\{Q_e\} = \alpha T_{air} \int_{area} \{N|_s\}\, d(area). \tag{20}$$

The governing Eqs. (3) and (4) can be expressed as

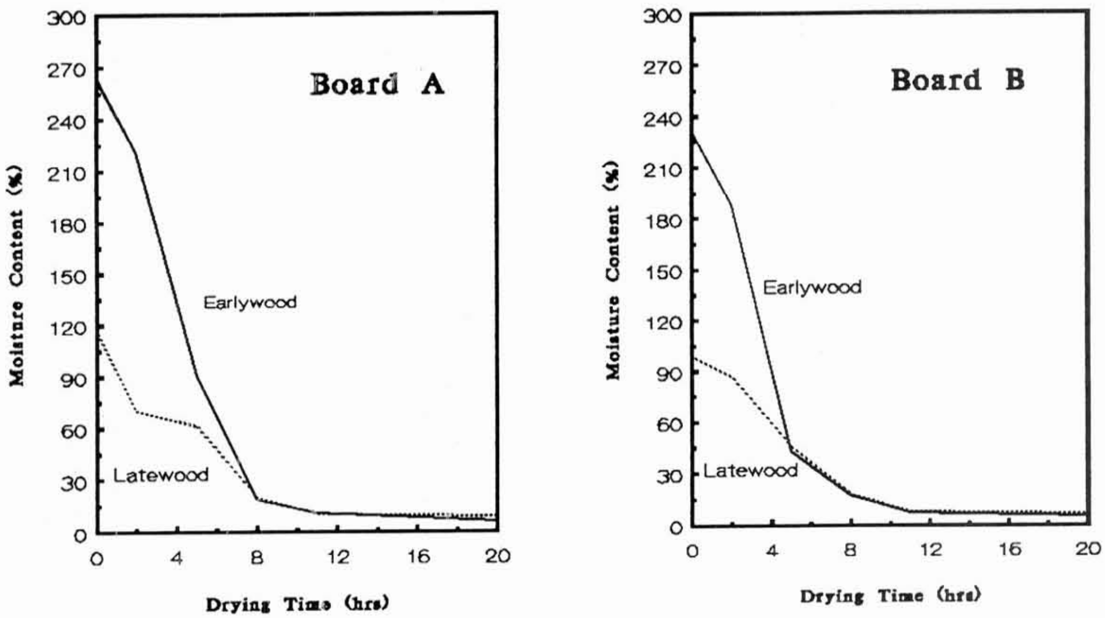

FIG. 3. Moisture content differences (radial direction) between earlywood and latewood during drying of southern pine.

as

$$[C_q]\{\dot{T}\} + [K'_{qq}]\{T\} = \{Q\}, \qquad (21)$$

and

$$[C_m]\{\dot{M}\} + [K'_{mm}]\{M\} = \{H\}. \qquad (22)$$

The simplified model has two-dimensional transfer directions at each node because transport behaviors in wood are field phenomena. For the transition transport, the governing equations are solved by an implicit direct integration scheme based on a modified Houbolt method (Kohnke 1989).

EXPERIMENT

To obtain the transport coefficients for southern pine, two southern pine boards [5.08 cm (T) by 15.24 cm (R) by 304.8 cm (L)] were dried using an air velocity of 5 m/sec, at 116 C dry-bulb and 71 C wet-bulb temperature. After the boards were dried for 2, 5, 8, and 11 hours, moisture gradients along the thickness (radial) directions were measured by the slicing method described by McMillen (1955). At each measuring time, a block (45.72 cm long) was sawn from each board and cooled in a freezer. Then two sections (2.45 cm long) were taken from the block. Ten wafers (0.508 cm thick) were cut from one of the sections to determine the moisture gradients along the thickness. To determine moisture gradient within each growth ring, the other section was cut to separate the earlywood and latewood of each growth ring.

Generally, the available data on heat and mass transport coefficients for the whole drying range are limited in the literature. However, Keylwerth (1952) reported a nearly complete list of properties for spruce. On the basis of the experimental data from this study and experimental work for spruce (Keylwerth 1952), the transport coefficients for southern pine and for spruce were derived over the entire drying range using Egner's method. Then, the functions K'_{qq} and K'_{mm} were approximated by three line segments as linearized functions for use in the FEM calculation. K'_{qq} is linear over the following temperature ranges: 0° to 86°; 86° to 110°; and $\geq$110°. K'_{mm} is linear over the moisture ranges: 0 to 36; 30 to 150; and $\geq$150.

TABLE 1. *Initial/boundary conditions and spruce properties used in the ANSYS FEM analysis.*

		Initial and boundary conditions	
Dry-bulb temperature = 110 C,		Wet-bulb temperature = 87 C	
Initial wood temperature = 10 C,		Temperature of air = 110 C	
Initial wood moisture potential = 86°M,		Moisture potential of air = 4°M	
Name	Unit	Thomas' Data	Data for ANSYS FEM
α_q	$W/m^2 \cdot K$	22.5	61.4 at T = 0°C 20.5 at T = 86°C 0.50 at T ≥ 110°C
α_m	$kg/m^2 \cdot sec \cdot °M$	2.5×10^{-6}	2.4×10^{-6} at °M = 0 3.1×10^{-6} at °M = 30 9.4×10^{-6} at °M ≥ 150
		Material properties of spruce	
K'_{qq}	W/mK	0.65	0.38 at T = 0 C 0.20 at T = 86 C 0.70 at T ≥ 110 C
K'_{mm}	$kg/m \cdot sec \cdot °M$	2.2×10^{-8}	2.2×10^{-8} at °M = 0 4.5×10^{-8} at °M = 30 7.3×10^{-8} at °M ≥ 150
C_q	$J/kg \cdot K$	2,500	2,500
C_m	kg (moisture)/ kg (dry body)°M	0.01	0.01

Figure 2 presents the moisture gradients that were measured along the thickness during drying. These experimental data were used to evaluate the transport coefficients. Data obtained during this study confirm published results that show a large difference in average moisture content between earlywood and latewood (Fig. 3).

NUMERICAL RESULTS

Results for spruce wood drying

The experimental results for drying spruce reported by Keylwerth (1952) have been used to compare different numerical solutions (Spolek and Plumb 1980; Thomas et al. 1980) and analytical results (Liu and Cheng 1989). In this study, the numerical solutions obtained from the ANSYS finite element program were compared with results from Keylwerth and Thomas. The initial and boundary conditions and the material properties are given in Table 1.

Figure 4 compares temperatures predicted by Thomas and by this finite element study with Keylwerth's experimental temperature data. In Fig. 5, Keylwerth's experimental moisture content values for spruce were compared with values calculated by Thomas and values predicted by this finite element study. As discussed by Thomas et al. (1980), the unusual shape of the surface MC experimental curve between t = 30 minutes and t = 200 minutes in Fig. 5a was not explained by Keylwerth (1952). The experimental data in this region were therefore considered to be suspect. In both comparison cases for moisture content and temperature, the solutions of this study are valid and approximate the experimental values more closely than Thomas' method.

Results for southern pine wood drying

Southern pine lumber contains layers of earlywood and latewood that have distinctly different physical properties for stiffness, resistance to mass flow, and thermal conductivity. These differences are most pronounced during the early stages of drying. Thus, an uneven flow

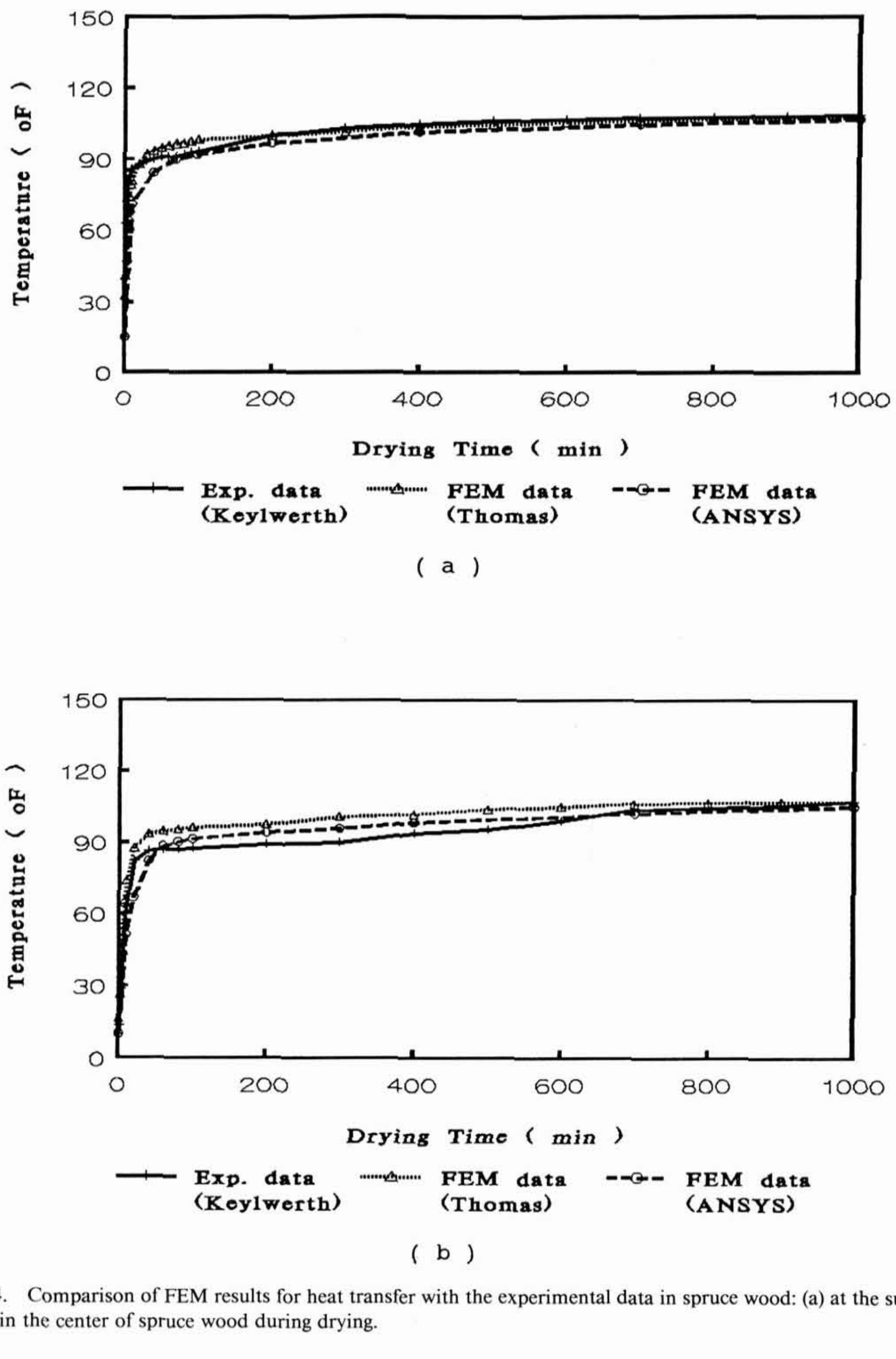

FIG. 4. Comparison of FEM results for heat transfer with the experimental data in spruce wood: (a) at the surface, and (b) in the center of spruce wood during drying.

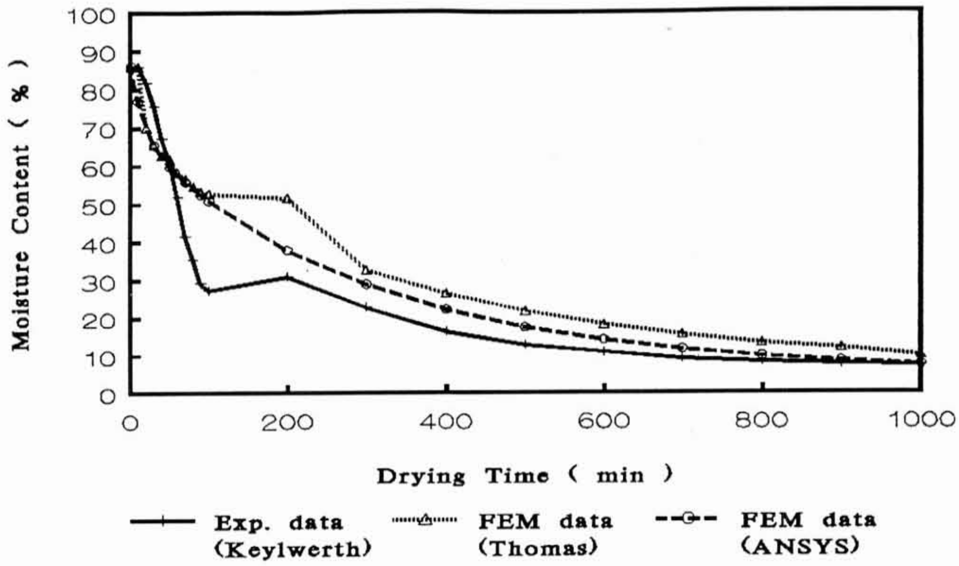

(a)

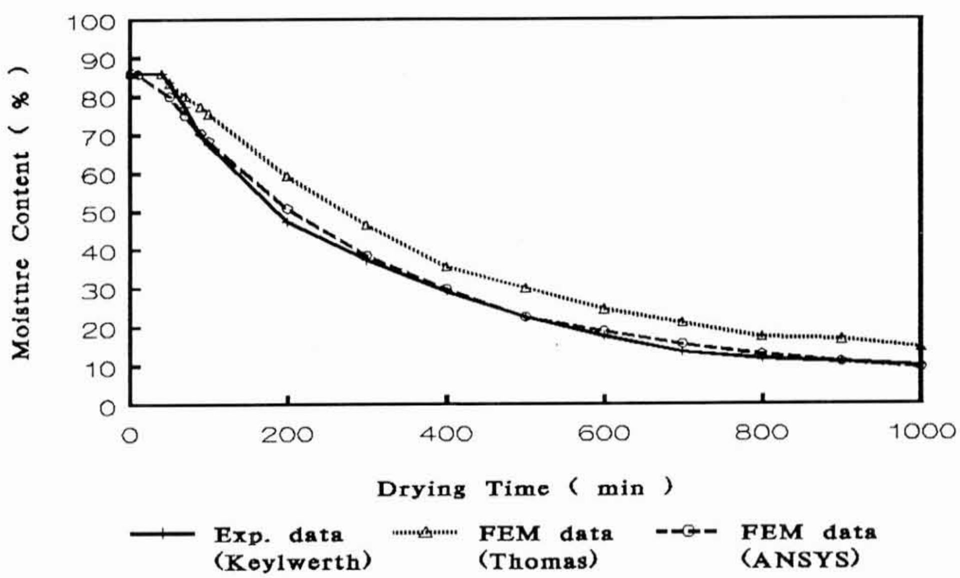

(b)

FIG. 5. Comparison of FEM results for mass transfer with the experimental data in spruce wood: (a) at the surface, and (b) in the center of spruce wood during drying.

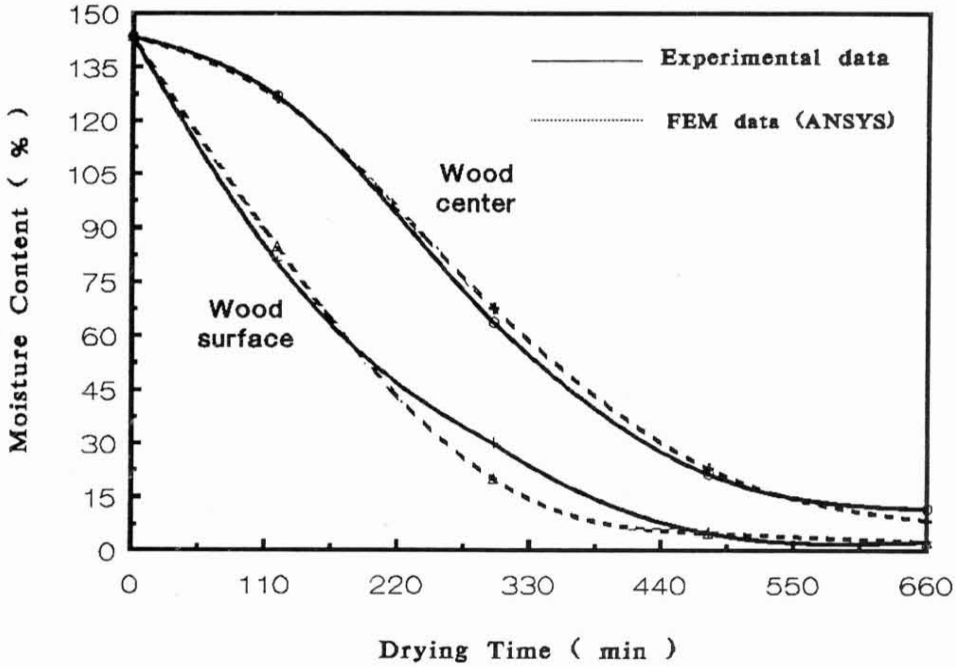

FIG. 6. Comparison of FEM results with the experimental data for drying of southern pine wood (radial direction).

of moisture and heat occurs that affects shrinkage and drying stresses. The initial and boundary conditions and the material properties used for the FEM analysis are shown in Table 2.

Thermal conductivity is much greater than mass conductivity in wood. Wood temperature quickly reaches an equilibrium during high temperature drying. Since drying-induced stresses and drying defects are related to the development of moisture gradients, this study

TABLE 2. *Initial/boundary conditions and southern pine properties used in the ANSYS FEM analysis.*

		Initial and boundary conditions	
Dry-bulb temperature = 115.6 C,		Wet-bulb temperature = 71.1 C	
Initial wood temperature = 10 C,		Temperature of air = 115.6 C	
Initial wood moisture potential = 143.57°M,		Moisture potential of air = 1.7°M	
Name	Unit		Data for ANSYS FEM
α_m	kg/m^2·sec·°M		4.0×10^{-5} at °M = 0 0.63×10^{-5} at °M = 30 0.10×10^{-5} at °M ≥ 150
		Material properties of southern pine	
Name	Unit	Earlywood	Latewood
ρ	kg/m^3	200	700
K'_{mm}	kg/m·sec·°M	9.8×10^{-8} 18×10^{-8} 18×10^{-8}	6.4×10^{-8} at °M = 0 7.5×10^{-8} at °M = 30 7.5×10^{-8} at °M ≥ 150
C_m	kg (moisture)/ kg (dry body)°M	0.01	0.01

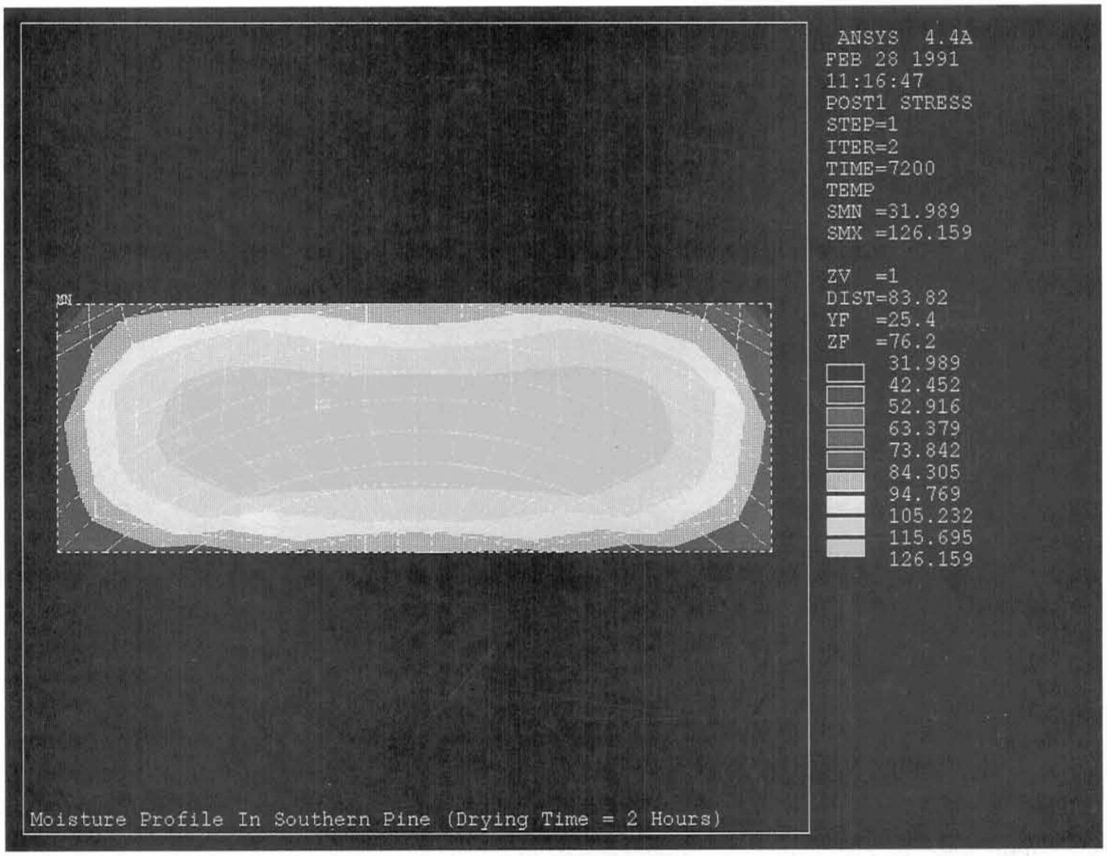

FIG. 7. FEM moisture profile in southern pine (drying time = 2 hours).

focuses on moisture movement in wood during drying. Figure 6 represents the comparison of the mass transfer of moisture from the FEM simulation with the experimental data. Figures 7 and 8 show the profiles of moisture across the board at different drying stages.

CONCLUSIONS

This study describes a way to apply the finite element method of analysis (FEM) to heat and mass transfer in wood drying. The main differences from previous studies are the inclusion of the influences of material differences between earlywood and latewood, consideration of transport coefficient variations over the whole range of the unsteady-state transport procedure, and the use of a dynamic nonlinear numerical technique to solve the transport governing equations. The transport coefficients, which are required for the FEM of analysis, are derived from experimental data.

Figures 7 and 8 indicate that the distributions of moisture content are influenced by the growth ring pattern. Since drying stresses are induced mainly by moisture gradients, FEM results indicate the drying stress pattern within wood. Using the FEM to predict transport gradients may lead to ways to modify drying schedules to minimize drying defects. Moisture content variations in a cross section of southern pine, as shown in Figs. 7 and 8, illustrate the ability of the FEM to incorporate differences in earlywood and latewood properties into the analysis.

Since these results agree with published experimental data even though the coupling terms

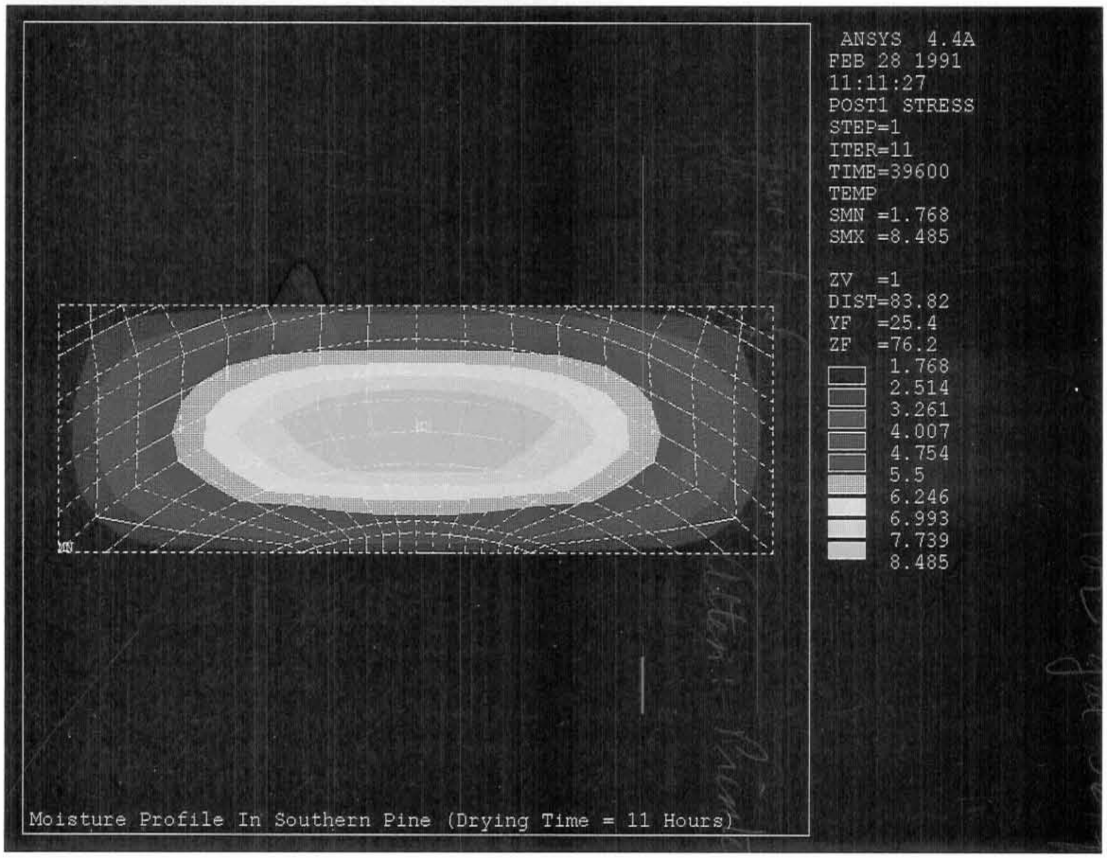

FIG. 8. FEM moisture profile in southern pine (drying time = 11 hours).

between heat and mass transfer are merged into the main transport coefficients, the coupling terms in the general governing equations apparently have small influence on the dynamic transport over the whole drying process.

ACKNOWLEDGMENT

Thanks are due the Mississippi Forest Products Laboratory and the Engineering Research Center at Mississippi State University for the support of this research. This study was supported under USDA Wood Utilization Research Grants.

REFERENCES

ASHWORTH, J. C. 1979. Design of drying schedules for kiln-drying of softwood timber. Development in drying, vol. 2. Hemisphere Publishing Corp., New York, NY.

EGNER, K. 1934. Beiträge zur Kenntnis der Feuchtigkeitsbewegung in Hölzern, vor allem in Fichtenholz, während der Trocknung unterhalb des Fasersättigungspunktes. Forschungsberichte Holz. Heft 2. 91 pp. Berlin, Germany (as cited by C. Skaar, 1954).

FELIXX S., J. C. RAZAFINDDRAKOTO, AND P. CASTERA. 1989. Modeling of hygrothermoelastic effects during timber drying. IUFRO Wood Drying Symposium, Seattle, WA.

HART, C. A. 1981. SIMSOR: A computer simulation of water in wood. Wood Fiber 13(1):46–71.

KAWAI, S., K. NAKATO, AND T. SADOH. 1979. Computation of drying stresses resulting from moisture gradients in wood during drying. II. Numerical calculation. Mokuzai Gakkaishi 25(4):272–279.

KEYLWERTH, R. 1952. Der Verlauf der Holztemperatur während der Furnier und Schnittholztrocknung. Holz Roh Werkst. 10(3):87–91.

KOHNKE, P. C. 1989. ANSYS theoretical manual. Swanson Analysis Systems, Inc., Houston, PA.

LESSARD, R. A. 1982a. A semi-empirical moisture transport model for on-line optimal lumber drying control. J. Dynamic Syst., Measurement, Control 104:277–282.

———. 1982b. A stress model for lumber drying control. J. Dynamic Syst., Measurement, Control 104:283–289.

LEWIS, R. W., K. MORGAN, AND H. R. THOMAS. 1979. Drying-induced stresses in porous bodies—An elasto-viscoplastic model. Computer Meth. Appl. Mech. Eng. 20:291–301.

LIU, J. Y., AND S. CHENG. 1989. Heat and moisture transfer in wood during drying. Proceedings, 3rd Joint ASCE/ASME Mechanics Conference, San Diego, CA. American Society of Mechanical Engineers. Pp. 79–85.

LUIKOV, A. V. 1964. Heat and mass transfer in capillary-porous bodies. Advances Heat Transf. Academic Press, New York, NY.

———. 1966. Heat and mass transfer in capillary-porous bodies. Pergamon Press, Oxford, UK 6:232–303.

———. 1975. System of differential equations of heat and mass transfer in capillary-porous bodies. Intl. J. Heat Mass Transf. (review) 18(1):1–14.

———, AND Y. A. MIKHAILOV. 1965. Theory of energy and mass transfer. Pergamon Press, Oxford, UK.

MCMILLEN, J. 1955. Drying stresses in red oak. Forest Prod. J. 5(1):71–76.

MOREN, T. J. 1989. Check formation during low temperature drying on Scots pine: Theoretical consideration and some experimental results. IUFRO Wood Drying Symposium, Seattle, WA.

MORGAN, K., H. R. THOMAS, AND R. W. LEWIS. 1982. Numerical modeling of stress reversal in timber drying. Wood Sci. 15(2):139–149.

MUJUMDAR, A. S., ed. 1980–1987. Advances in drying, vols. 1–4. Hemisphere Publishing Corp., New York, NY.

NORTHWAY, R. 1989. Moisture profiles and wood temperature during very high temeprature drying of *Pinus radiata* explain lack of degrade. IUFRO Wood Drying Symposium, Seattle, WA.

PLUMB, O. A., C. A. BROWN, AND B. A. OLMSTEAD. 1984. Experimental measurements of heat and mass transfer during convective drying of southern pine. Wood Sci. Technol. 18:187–204.

RICE, R. 1988. Mass transfer, creep and stress development during the drying of red oak. Ph.D. dissertation, Virginia Polytechnic Institute and State University, Blacksburg, VA.

SIAU, J. F. 1984. Transport processes in wood. Springer-Verlag, New York, NY. 245 pp.

SKAAR, C. 1954. Analysis of methods for determining the coefficient of moisture diffusion in wood. Forest Prod. J. 4(6):403–410.

———. 1988. Wood-water relations. Springer-Verlag, Berlin, Germany. 283 pp.

SPOLEK, G. A., AND O. A. PLUMB. 1980. A numerical model of heat and mass transport in wood during drying. Drying 1980, vol. 2. Sec. II:84–92.

THOMAS, H. R., R. W. LEWIS, AND K. MORGAN. 1980. An application of the finite element method to the drying of timber. Wood Fiber 11(4):237–243.